RESEARCH PAPER

EphA2 Targeting Pegylated Nanocarrier Drug Delivery System for Treatment of Lung Cancer

Apurva R. Patel • Mahavir Chougule • Mandip Singh

ABSTRACT

Purpose Evaluation of tumor targeting pegylated EphA2 peptide coated nanoparticles (ENDDs) of a novel anticancer agent DIM-C-pPhC$_6$H$_5$ (DIM-P) and Docetaxel (DOC) and investigate its antitumor activity and potential for treatment of lung cancer.
Methods Nanoparticles were prepared with DIM-P and DOC (NDDs) using Nano-DeBEE. ENDDs were prepared by conjugating NDDs with 6His-PEG2K-EphA2 peptide and characterized for physicochemical properties, binding assay, cytotoxicity, cellular uptake studies, drug release and pharmacokinetic parameters. Anti-tumor activity of ENDDs was evaluated using a metastatic H1650 and orthotopic A549 tumor models in nude mice and tumor tissue were analyzed by RT-PCR and immunohistochemistry.
Results Particle size and entrapment efficiency of ENDDs were 197 ± 21 nm and 95 ± 2%. ENDDs showed 32.5 ± 3.5% more cellular uptake than NDDs in tumor cells. ENDDs showed 23 ± 3% and 26 ± 4% more tumor reduction compared to NDDs in metastatic and orthotopic tumor models, respectively. *In-vivo* imaging studies using the Care stream MX FX Pro system showed ($p < 0.001$) 40–60 fold higher flux for ENDDs compared to NDDs at tumor site.
Conclusions The results emanating from these studies demonstrate anti-cancer potential of DIM-P and the role of ENDDs as effective tumor targeting drug delivery systems for lung cancer treatment.

A. R. Patel • M. Singh (✉)
College of Pharmacy and Pharmaceutical Sciences, Florida A&M
University, Tallahassee, Florida 32307, USA
e-mail: mandip.sachdeva@gmail.com

M. Chougule
College of Pharmacy, University of Hawaii at Hilo, Hilo
Hawaii 96720, USA

ABBREVIATIONS

DIM-P	DIM-C-pPhC$_6$H$_5$
Doc	Docetaxel
DOGS-NTA-Ni	1,2-dioleoyl-sn-glycero-3-[(N-(5-amino-1-carboxypentyl) imidodiacetic acid) succinyl nickel salt]
DSC	Differential Scanning Colorimetry
ENDDs	EphA2 peptide coated nanoparticles
His	Histidine
Nano-luc	Luciferin containing NDDs
Nano-luc-EphA2	Luciferin containing ENDDs
NCs	Nanolipidcarriers
NDDs	Nanoparticles with DIM-P and
NDi	Nanoparticles with DIM-P
NDo	Nanoparticles with Doc
NSCLC	non small cell lung cancer
PEG2K	Polyethylene Glycol (2,000 daltons)
TPGS	D-alpha tocopheryl polyethylene glycol 1,000 succinate

INTRODUCTION

Despite an increased understanding of the pathogenetic mechanisms underlying lung cancer and the advent of several new chemotherapeutic regimens, the success rate in the treatment of NSCLC is not impressive (1). Conventional treatments (surgical resection, radiation, and chemotherapy) are not satisfactory based on survival rate of cancer patients. Despite recent advances in chemotherapy, current therapeutic options are relatively ineffective (survival rates in NSCLC remain <50% and an advanced stage IV cancer patient has a survival rate of <20%) (2). Systemic or oral drug deliveries are

not often successful due to a limited amount of the anticancer drug reaches the lung tumor site and administering a high dose of anticancer drug is associated with adverse side effects (3). Therefore, site-specific targeted delivery of anticancer drugs to the tumor site is the most crucial step for effectively treating lung cancer and increasing the survival rate in patients. Studies conducted in our and other laboratories have shown that DIM-P, a PPAR-γ agonist induces antitumor effects in variety of cancer types including lung cancer with minimal or no toxicity (4–8). Doc is an anti-microtubular first-line chemotherapeutic agent in treatment of NSCLC (9). Our preliminary data strongly demonstrates that DIM-P in combination with Doc exerts synergistic (*in vitro*) and additive (*In vivo*) anticancer activity against lung cancer. The combination effects involve activation of growth inhibitory and proapoptotic proteins and inhibition of anti-apoptotic proteins (5). Standard Chemotherapy consists of a combination of two anticancer drugs, generally cisplatin or carboplatin and paclitaxel or gemcitabine or Doc (1,10) and most of these agents show several adverse side effects (2). Doc is a semi-synthetic taxoid derived from 10-deacetyl bacatin III which stabilize microtubule by promoting the assembly of microtubules and inhibiting the depolymerization of tubulin. Doc showed potent anticancer activity as a single agent or in combination therapy with cisplatin in advanced NSCLC (9).

Marketed pharmaceutical formulations used Cremophor EL and Tween 80 (combined with ethanol) as vehicles for paclitaxel and Doc administration, which have several adverse effects (11,12). Nanotechnology-based formulations such as polymer conjugates, polymeric micelles, liposomes, or nanoparticles *e.g.* Abraxane (13,14) and chitosan oligomer colloidal carriers (15) have been studied to overcome problems associated with conventional formulations. Another approach is to employ a tumor-specific ligand for more specific recognition of and interaction with cancer cells and reduce the side effects of drugs on normal cells. Therefore, to improve clinical use of Doc, there is need for development of actively targeted nanotechnology based formulations.

Lipid nanoparticles are emerging drug carrier system for treatment of cancer (16). Development of a stable biodegradable targeted nanoparticle based delivery system which simultaneously delivers synergistically acting DIM-P and Doc locoregionally to lung tumor cells exerting significant antitumor activity with minimizing Doc toxicity will be beneficial for treatment of lung cancer and lung metastases. Furthermore, selective targeting of this delivery system to EphA2 receptor over-expressing lung tumor cells will significantly enhance effectiveness of this approach. Several other researchers have also shown overexpression of EphA2 receptor in different tumor cells (17–20). An Eph family receptor tyrosine kinase (RTK) and ephrin ligands have been linked to many types of cancers, including glioblastoma, melanoma, breast, colorectal, bladder, NSCLC, prostate and ovarian carcinomas (21–24).

Along with EphA2, ephrinA1 are responsible for the development and continuation of many different tumors (19). Moreover, the level of EphA2 expression correlates with tumor malignancy and poor patient survival (21,23). Recent studies suggests strong involvement of EphA2 expression in tumorigenesis, including metastasis, angiogenesis, and invasion (25,26).The role of EphA2/ephrinA1 in tumorigenesis/progression is multifaceted and depends on variables such as cell type and microenvironment. These involves the expression of the EphA2, signaling pathways and the effect of the signaling on the tumor cells. Due to EphA2/ephrinA1 expression and diversified functions, they are widely studied for their involvement with tumorigenesis, angiogenesis and metastasis *etc*. The EphA2 overexpression is found to be involved in malignancy in a non–tyrosine-phosphorylated state (27), where as hyper-phosphorylation and constitutive activation are common traits for RTKs to involve in tumorigenesis. Also, the phosphorylation-independent effects of EphA2 with the cytoplasmic domain plays a role in tumorigenesis (19). Targeted nanoparticles can incorporate multiple functions into the particles and have tremendous potential to improve the current clinical paradigms of cancer therapeutics (13,14). An approach for targeting EphA2 expressing tumor cells includes use of Eph specific antibody and antagonistic peptides that display selective binding. Recently, a polypeptide (GGGGYSAYPDSVPMMSK) was used as a targeting ligand to deliver magnetic nanoparticles selectively to ovarian cancer cells overexpressing EphA2 receptors (28). The center of the peptide [YSAYPDSVPMMS (YSA)] was found to bind specifically to EphA2 receptor using the YPDSVP region by mimicking as an ephrin (29). Also, targeting to EphA2 receptor over-expressing prostate (30) and ovarian (31) cancers has been studied using monoclonal antibodies which demonstrated inhibition of growth, migration and invasiveness. The delivery of drugs containing nanoparticles targeting EphA2 receptor for treatment of lung cancer has not been investigated. The objective of this study is to develop Epha2 receptor targeted delivery system of DIM-P and Doc based on nanotechnology for the treatment of lung cancer (Fig. 1). The results from these studies will allow translating this combination to the cancer patients with improved clinical outcome.

MATERIALS AND METHODS

Materials

DIM-P was synthesized as described previously (32). The triglycerides Miglyol 812, Compritol 888 ATO, Dynasan 118, Precirol, Gleol, Monosterol, Lebrasol and Transcutol were from Sasol Germany GmbH (Witten, Germany) and Gattefosse (Saint Priest, France). 1,2-dioleoyl-sn-glycero-3-[(N-(5-amino-1-carboxypentyl) imidodiacetic acid) succinyl
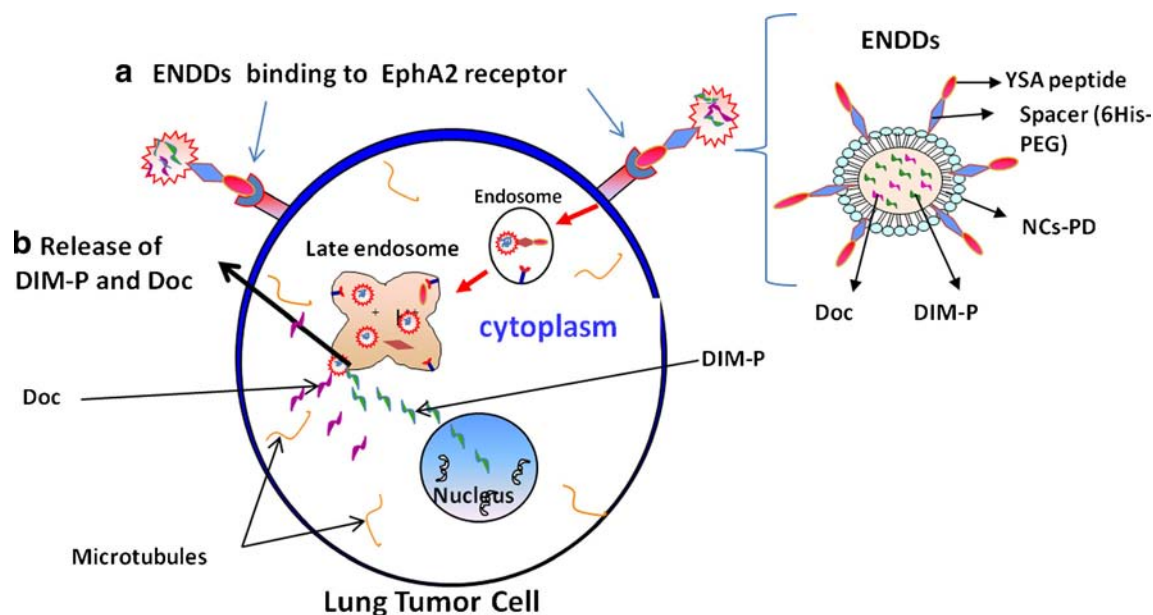
Fig. 1 Schematic of ENDDs and ENNDs uptake *via* EphA2 receptor medicated endocytosis (**a**) and release of DIM-P/Doc in cytoplasm (**b**) to exert anticancer activity.

nickel salt] (DOGS-NTA-Ni) was purchased from Avanti Polar lipids (Alabaster, USA). Fetal bovine serum (FBS), antibiotics mix and lipophilic fluorescent dyes (DIO dye and DID-oil) were from Invitrogen Corp (Eugene, OR). The A549 and H1650 human NSCLC cell line were obtained from American Type Culture Collection (Rockville, MD, USA). Cells were grown in RPMI, F12K/DMEM mediums (Sigma, St. Louis, MO, USA) supplemented with 10% FBS and antibiotic mixture. The cells were maintained at 37°C in the presence of 5% CO2 in air. All other chemicals used in this research were of analytical grade. The six histidine tagged PEGylated YSA (6His-PEG-YSA) tumor homing peptide and control non specific peptide YKA (6His-PEG-YKA) peptide were synthesized by GenScript Corporation (NJ, USA).

Animals

BALB/c mice (20–30 g) and Nu/nu mice (20–30 g) (Charles River Laboratories, Wilmington, MA, USA) were used for the animal studies. The protocols were approved by the Institutional Animal Care and Use Committee at Florida A & M University. Animals were given standard animal diet and kept in a climate controlled room (22±1°C @ 35–50% relative humidity) during the experiments.

Preparation and Optimization of NDi, NDo & NDDs

Nano-lipid carriers (NCs) were prepared by modified hot melt homogenization (33) using triglycerides and optimized process variables. Briefly, DIM-P and Doc were dispersed in organic solvent. To the resultant organic phase miglyol or mixture of transcutol & miglyol (1:1) and DOGS-NTA-Ni were added

and organic solvent was evaporated. To this, a mixture of gleol and monosteol (4:3) were added. An aqueous phase consisting of Lutrol® F68 (1% w/w), and span 80 (0.5% w/w) in distilled water was added to lipid phase under high speed mixing (20,000 rpm for 15 min) followed by passing through Nano DeBee®(BEE International, Inc, MA, USA) at 20,000–30,000 psi for 3 to 5 cycles. NCs for imaging were prepared by adding DID dye to organic phase during the preparation NCs. Similarly, for *in-vivo* animal imaging, D-luciferin loaded NCs for bioluminescent imaging were prepared.

Factors such as lipid to oil ratio, drug loading and homogenization time were optimized to get nanoparticles of desired characterization parameters, such as particle size, polydispersity index (PDI), zeta potential and encapsulation efficiency. The Nicomp 380 ZLS (Particle Sizing Systems, Port Richey, FL) was used to measure particle size and zeta potential of NDs or ENDDs. The drug loading and entrapment efficiency were determined as reported earlier (33).

Formulations were lyophilized at −70°C and 100 milliTorr vacuum pressure (SMART Freeze Drying, FTS Systems, SP Scientific, USA) using different cryoprotectants (trehalose, mannitol and sucrose) and trehalose was selected. Formulations were lyophilized using 5% w/v trehalose (cryoprotectant) and viscosity of the NDDs formulations were adjusted to 2.5–3 cP by resuspending the lyophilized formulation in Vitamin E TPGS (2%) aqueous sterile solution prior to use.

Preparation of ENDDs

To prepare ENDDs, 200 μl of NDDs were mixed with 50 μl of 6-Histidine -tagged PEGylated (PEG-2000) EphA2 peptide

aqueous solution (5 mg/ml) and incubated for 60 min at room temperature. The free peptide was separated using a Spin-OUT column (molecular weight cut off of 10,000 Da, Geno Technology Inc., USA).

In-Vitro **Characterization**

In-vitro drug release of DIM-P solution, Doc solution, NDi, NDo, NDDs and ENDDs were carried out as described previously (34) using phosphate buffer saline (PBS) containing 2.5% w/v Volpo-20 & 2.5% TPGS as dissolution medium. At different time points, sample was collected and amount of DIM-P and Doc released was determined using HPLC. The interaction of DIM-P and Doc with lipids and association of DIM-P and Doc in NDs formulations were determined using a DSCQ100 (TA instrument, DE) (34). Freeze-dry NDDs were stored at 4°C and also at room temperature (mean temperature being 25.7 ± 0.6°C) for three month. Aliquots were removed after intervals of time and analyzed for particle size, entrapment efficiency, release rate and DIM-P content by methods mentioned above. The slope of the log percent DIM-P and Doc remaining vs time plot curve was used to determine degradation rate constant (K) using Eq. (1).

$$Slop = k/2.303 \tag{1}$$

Where, K is the degradation rate constant.

In-Vitro **Analysis**

a) **Binding assay:** The binding assay was carried out as reported (35) to determine the peptide to DOGS-NTA-Ni ratio.
b) **Cytotoxicity:** *In-vitro* cytotoxicity of DIM-P and Doc formulation was carried out in A549 cell lines using crystal violet dye assay as reported (5). Briefly, 10^4 cells/well were plated in 96 well plate and treated with different concentration of DIM-P, Doc, NDi, NDo, NDDs and YSA peptide. After 72 h cells were washed with PBS and cell viability was measured by crystal violet assay.
c) **Cellular Uptake study:** Internalization of the ENDDs formulations was studied by incubating ENDDs and negative controls (NDDs) with A549 cells for 2 h at 37°C followed by washing to remove unbound NCs. The associated fluorescence was evaluated by microscopy.

Pharmacokinetic Analysis of NDs

Pharmacokinetics of DIM-P and Doc in BALB/c mice were determined following I.V. administration of NDi, NDo, NDDs & ENDDs (DIM-P equivalent to 5.0 mg/kg, Doc equivalent to 10.0 mg/kg). Animals were randomly distributed into experimental groups ($n=6$) and fasted overnight prior to experiment. Blood samples (250 µL) were collected by heart puncture at the following time points: 0, 0.017, 0.25, 0.5, 0.75, 1, 3, 6, 8, 12 and 24 h. Samples were processed and extracted drug was analyzed by HPLC analysis (36). Briefly, DIM-P was separated from plasma by protein precipitation using acetonitrile and samples were centrifuged for 15 min at 10,000 g. Sample was run on a mobile phase consisting of acetonitrile and water (90:10% v/v) using a Waters Symmetry® C18 guard column (5 µm, 3.9×20 mm) and a Waters Symmetry® C18 column (5 µm, 4.6×250 mm) at a flow rate of 1.0 mL/min and DIM-P was monitored at 242 nm. Pharmacokinetic parameters were calculated using non-compartmental techniques with WinNonlin® 5.0 software (Pharsight Corporation, Mountain View, CA, USA).

In Vivo Anticancer Evaluation in Lung Cancer Models

To evaluate *in-vivo* anticancer activity of ENDDs, orthotopic A549 cell tumor model (5) was developed as reported earlier and H1650 cells were injected *via* tail vein to develop the metastatic tumor model (33). Ten days after tumor implantation, mice were randomly divided into the following groups ($n=10$) to receive various DIM-P and Doc formulations; A) control group received vehicle (placebo ENDDs); B) NDi (DIM-P equivalent of 5 mg/kg) every fifth day; C) NDo (Doc equivalent of 2 mg/kg) every fifth day; D) NDDs (DIM-P equivalent of 5 mg/kg and Doc equivalent of 2 mg/kg) every fifth day; E) ENDDs (DIM-P equivalent of 5 mg/kg and Doc equivalent of 2 mg/kg) every fifth day. After 28 days, all animals were sacrificed and tumor tissues with lung were collected. The lung weights and tumor volume were used for assessment of the therapeutic activity. Some of the tumors were fixed in formalin and some were rapidly frozen in liquid Nitrogen and stored in -80°C for RT-PCR analysis.

RT-PCR Analysis

Total RNA was extracted from tumor tissue using RNeasy kit followed by conversion to complementary DNA using qPCR Mastermix as per the manufacturer's protocol. An ABI 7300 RT-PCR (Applied Biosystems, Carlsbad, CA, USA) was used for amplification and a PCR array data analysis software (SABiosciences, Valencia, CA, USA) was used to determine changes in the mRNA levels of PARP, caspases, Bcl-2, Bax, BAD, Mcl-1, survivin, NF-κB and β-actin as a control.

In-Vivo Imaging of Tumors and Tracking of NDDs & ENDDs

Imaging of tumors and tracking of NDDs & ENDDs was performed using Carestream *In-Vivo* MS FX PRO using bioluminescence imaging, which is based on the introduction and

Table I Effect of Lipid to Oil Ratio on the NDDs. Values are Expressed as Mean SD ($n = 6$)

Lipid:Oil	Size (nm)	PDI	Zeta potential (mV)	% Encapsulation efficiency
3:1	301 ± 14.23	0.353 ± 0.05	28.0 ± 3.0	69.19 ± 7.76
1:1	200 ± 16.36	0.327 ± 0.09	25.0 ± 2.0	75.33 ± 02.02
2:1	**175 ± 11.55**	**0.174 ± 0.02**	**24.9 ± 4.0**	**95.03 ± 03.75**
1:2	372 ± 14.52	0.475 ± 0.08	28.0 ± 6.0	42.22 ± 11.34

The desired values are represented in bold

expression of a gene construct to produce a protein "luciferase", using 4T1-luc2 orthotopic tumor model. NDDs & ENDDs were injected by tail vein into the tumor bearing mice. Following the injection, imaging of whole body and tumor area of animals were done at 0, 0.017, 0.25, 0.5, 1, 2, 3, 6, 8, 12 & 24 h. time points. Mice were anesthetized with 2% isoflurane using a 1 L/min O2 flow rate and placed in the prone position in the *In-Vivo* MS FX PRO. Bioluminescent imaging was performed using 745 nm excitation and 800 nm emission wavelengths. A 13 cm field of view (FOV) was used for whole body imaging and 6.6 cm for high resolution imaging of the tumor area. Targeting to the tumor vasculature by NDDs & ENDDs was quantified by drawing a region of interest (ROI) around the tumor area and measuring bioluminescence as total radiant efficiency, $[p/s]/[\mu W/cm^2]$.

Statistical Analysis

Analyzed data were represented as mean ± standard deviations (SD) and model parameters as estimates with ± standard errors (SE). Significance between two groups was measured by student's *t* test and between three or more groups by one-way variance analysis (ANOVA); data were explored for two-way ANOVA analyses where applicable. Probability (*p*) values < 0.05 were considered significant. All statistical analyses were performed using GraphPad Prism® 5.0 software (San Diego, CA).

RESULTS

Preparation and Optimization of NDDs

The different ratio of lipid to oil had a significant impact in the formulation of NDDs (Table I). The decrease in lipid concentration led to significant reduction in the particle size and PDI but an increase in the encapsulation efficiency was observed. Furthermore, it was observed that encapsulation efficiency was decreased with reduction in oil concentration. The effect of drug loading on the physicochemical properties of NDDs is shown in Table II. The increase in the drug loading was related to decrease in encapsulation efficiency with increases in the particle size and PDI. Homogenization pressure/cycle was considered as an important parameter for optimization of the nanoparticle. As shown in Table III, a significant decrease ($p < 0.05$) in the particle size was observed with increase in the pressure with simultaneous decrease in the encapsulation efficiency. Final formulation used for *in-vivo* study is shown in Table S1.

For longer storage and stability the prepared NDDs were freeze dried. Preliminary screening experiments were carried out using different cryo-protectants and trehalose was found to be most optimum in maintaining the original properties of formulations. The ratio of the particle size after and before freeze drying was found to be about 1. Which indicates that there is non-significant change upon reconstitution of formulations. Also, the freeze dried cake formed was fluffy in nature and easily redispersible in less than 30 s.

Preparation and Characterization of ENDDs

The ENDDS formulation prepared using triglycerides had a particle size of 190 ± 17 nm and polydispersity of 0.21 ± 0.06. The zeta potential of ENDDs formulations in distilled water was −27.38 ± 2.98. The total DIM-P and Doc content assay results indicated that

Table II Effect of Drug Loading on the NDDs. Values are Expressed as Mean SD ($n = 6$)

Drug loading	Size (nm)	PDI	Zeta potential (mV)	% Encapsulation efficiency
5%	157 ± 06.35	0.198 ± 0.03	28.4 ± 4.6	94.03 ± 3.34
10%	**197 ± 08.67**	**0.261 ± 0.02**	**28.8 ± 3.2**	**92.91 ± 1.67**
15%	263 ± 21.72	0.377 ± 0.07	27.8 ± 5.7	75.37 ± 3.04
20%	342 ± 20.29	0.456 ± 0.07	29.0 ± 5.2	58.82 ± 7.65

The desired values are represented in bold

Table III Effect of Pressure (psi)/Cycle on the NDDs. Values are Expressed as Mean SD ($n = 6$)

| Pressure (psi)/cycle	Size (nm)	PDI	Zeta potential (mV)	% Encapsulation efficiency
10,000/5	242 ± 04.97	0.426 ± 0.03	27.2 ± 3.5	90.85 ± 02.5
15,000/5	197 ± 10.42	0.259 ± 0.04	27.9 ± 3.3	83.04 ± 04.4
20,000/5	**190 ± 08.56**	**0.198 ± 0.06**	**28.5 ± 4.2**	**92.28 ± 03.8**
30,000/5	142 ± 09.55	0.302 ± 0.05	29.0 ± 3.6	74.89 ± 02.2

The desired values are represented in bold
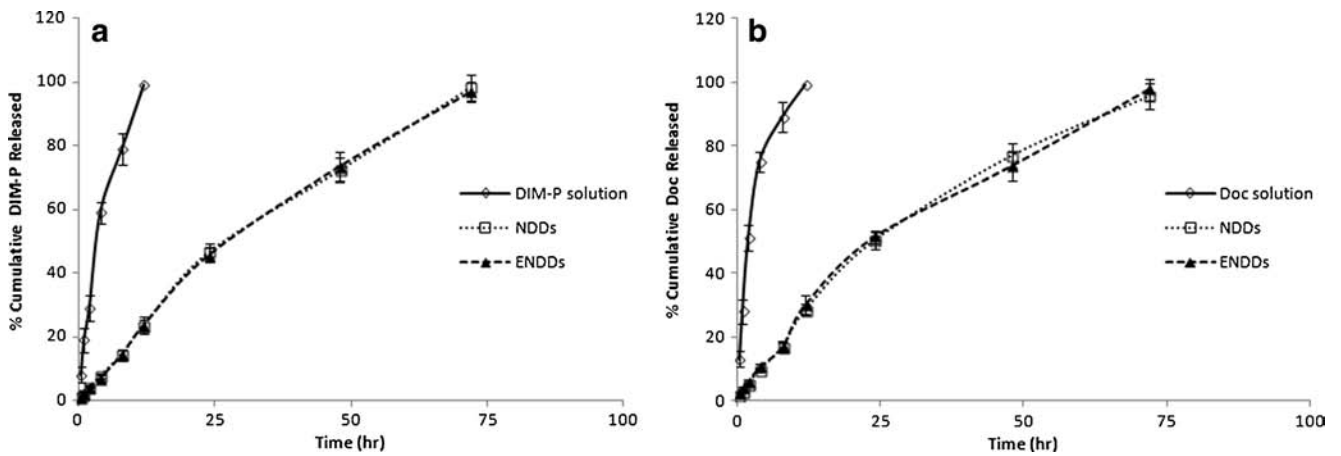
Fig. 2 *In-Vitro* Release Study of (**a**) DIM-P and (**b**) Doc from NDDs, ENDDs and DIM-P/Doc Solution.

approximately 4.72 ± 0.3 mg/ml of DIM-P and 1.87 ± 0.1 mg/ml of Doc was present in the ENDDs formulation.

The entrapment efficiency (EE) of formulations was more than 95%.

Fig. 3 Differential Scanning Calorimetry of DIM-P/Doc formulations. (**a**) DIM-P alone, (**b**) Doc alone, (**c**) Gleol + Miglyol, (**d**) blank NDDs formulation 5) NDDs formulation.
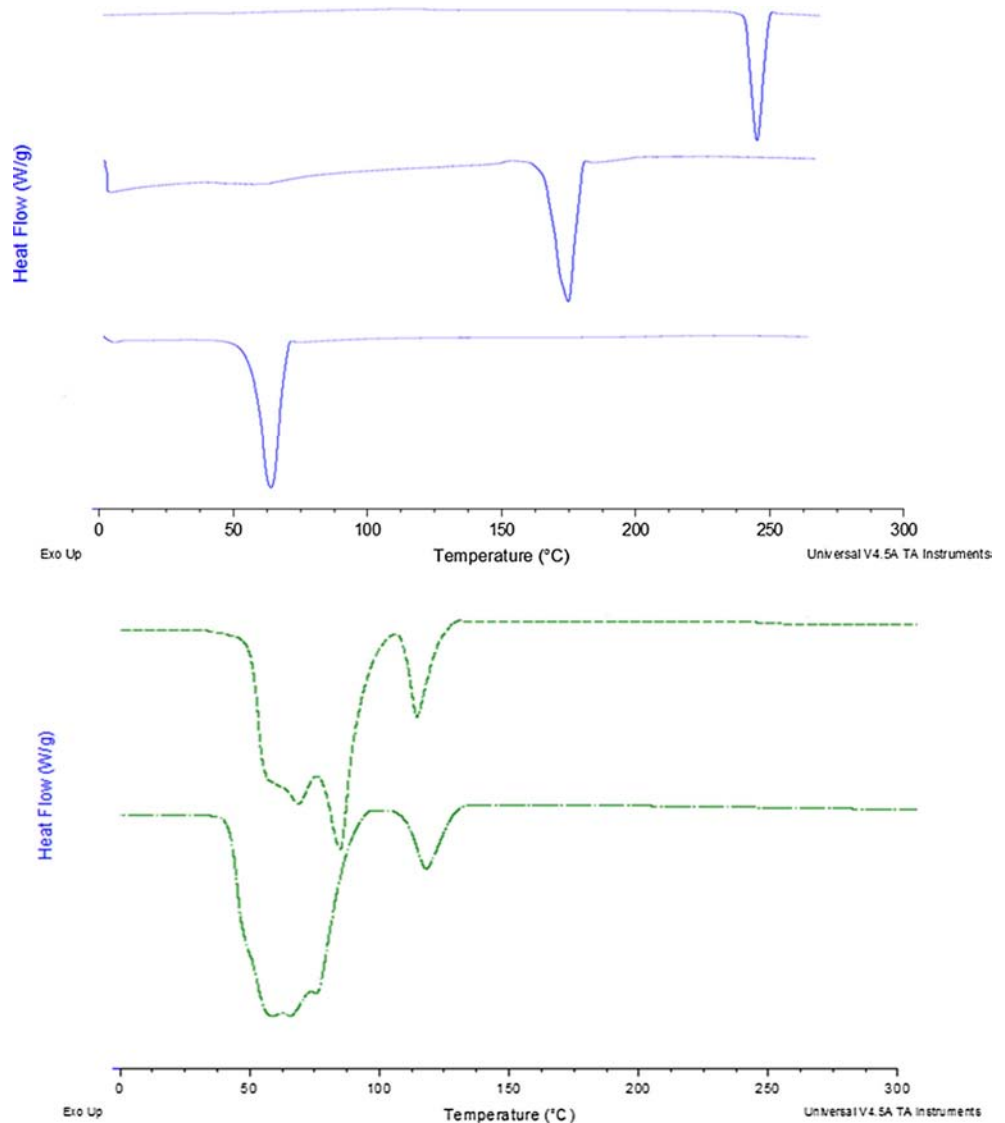
Table IV *In Vitro* Cytotoxicity of DIM-P, Doc and ENDDs Formulations Against A549 Cells

	DIM-P	Doc	DIM-P+Doc	NDi	NDo	NDDs
IC$_{50}$ (μM)	6.8 ± 0.7	0.02 ± 0.01	3.8 ± 0.6 (DIM-P) + 0.009 ± 0.001 (Doc)	6.9 ± 0.9	0.02 ± 0.01	3.9 ± 0.5 (DIM-P) + 0.01 ± 0.01 (Doc)

In-Vitro Characterization

USP dissolution apparatus was used to evaluate *in-vitro* release of DIM-P and Doc from nanoparticle formulations. We used 2.5% w/v Volpo-20 and 2.5% w/v TPGS in phosphate buffer as a dissolution medium to maintain the sink conditions based on the solubility of DIM-P and Doc. At initial 8 h, NDDs formulation released 8% of DIM-P and 46% after 24 h. At the end of 72 h, total of >95% of DIM-P was released from NDDs formulation. There was non-statistical difference between release of DIM-P from NDDs and ENDDs. Figure 2 reveals the *in vitro* drug release profiles of Doc from NDDs and ENDDs sustained the drug release with 45% of drug in 24 h. The NDDs and ENDDs formulations were able to release the DIM-P and Doc in controlled manner and more than 95% of drug was released after 72 h (Fig. 2). The DSC thermograms of DIM-P, Doc, and NDDs are represented in Fig. 3. For the free DIM-P and Doc, the thermogram revealed a small, clear event at about 250°C and 170°C (Fig. 3), a characteristic crystalline form melting peak. The DSC thermogram of gleol

Fig. 4 Cellular uptake study, microscopic images: fluorescent images of (**a**) ENDDs, (**b**) NDDs containing DiO dye after 2 h of incubation with A549 cells and (**c**) quantification of cellular uptake of fluoresce. Three different area were photographed for three different expeiments and images were analyzed by ImageJ. Data represented as mean ± SD. (*n* = 9) (*, *p* < 0.05, significantly different).
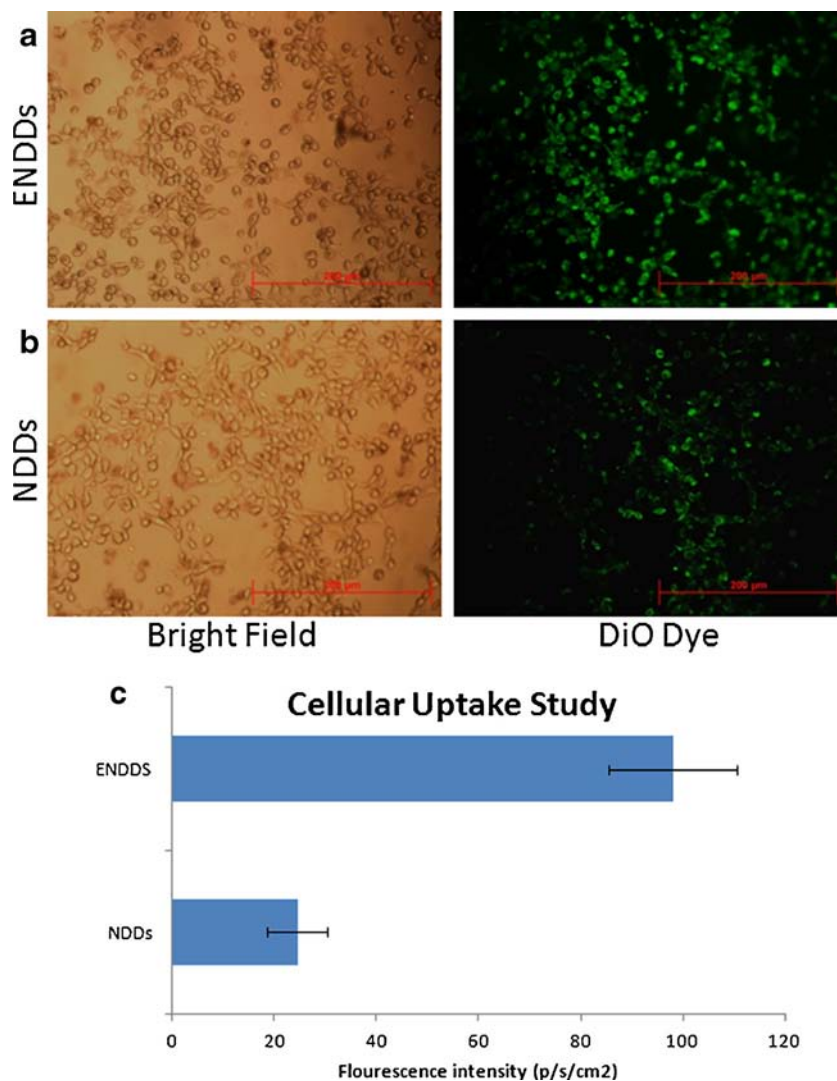
and monosteol showed a sharp endothermic peak at about 63°C. Furthermore, the thermal analysis of NDs formulation also showed disappearance of sharp DIM-P/Doc endothermic peak (Fig. 3). The main advantage of NDs nanoparticle is presence of oil which helps to hold higher amount of drug and stabilize the nanoparticles. Freeze dried NDDs were found to be stable and there were no significant changes observed in the encapsulation efficiency, particle size and PDI before and after storage of 3 months at 4°C and at room temperature.

In-Vitro Analysis

a) **Binding assay:** The binding affinity of peptide to DOGS-NTA-Ni was evaluated at different amounts (6.25 µg, 12.5 µg, 25 µg and 50 µg) of EphA2 peptide (Fig S1). With increase in EphA2 peptide (25 µg) the shift in fluorescence intensity was increased more than 80 times and further increase in EphA2 peptide concentration was not significantly increasing the shift in fluorescence intensity. On the other hand, incubation of ENDDs prepared without DOGS-NTA-Ni spacer at any concentration of EphA2 peptide did not show any fluorescence shift.

b) **Cytotoxicity:** The DIM-P and Doc showed IC50 value of 6.8 and 0.02 µM against A549 cells respectively. The NDi, NDo, showed comparable IC50 value to DIM-P and Doc with no statistical differences ($p > 0.05$) against A549 cells, suggesting that DIM-P and Doc was still active

when entrapped in nanoparticles (Table IV). The NDDs showed decrease in IC50 value to DIM-P and Doc with statistical differences ($p > 0.05$) against A549 cells, suggesting that DIM-P and Doc was acting synergistically when entrapped in ENDDs. The placebo NDs showed >98% viability of A549 cells demonstrating non-toxicity and safety of excipients used in development of nanoparticle system. Also, we monitored the cytotoxicity of YSA peptide and Blank ENDDs and cell viability was more than 90% at 300 um concentration.

c) **Cellular Uptake study:** The cellular uptake studies showed the effective internalization of NDDs and ENDDs within A549 cells in 2 h (Fig. 4). The intensity of fluorescence was significantly lower by 4 fold in case of NDDs as compared to ENDDs.

Table V Pharmacokinetic Parameters for DIM-P Estimated from Non-Compartment Analysis Following i.v. Administration (5.0 mg/kg Equivalent of DIM-P) in Rats

	DIM-P Solution	NDDs	ENDDs
AUC_{0-24} (ug.hr)/ml	124.22 ± 13.65	378.35 ± 95.78	664.17 ± 135.89
K10-HL (hr^{-1})	2.98 ± 0.65	7.07 ± 0.39	7.56 ± 0.95
Cmax (ug/ml)	216.25 ± 23.59	265.32 ± 29.51	320.26 ± 30.21
Cl (ml/kg/h)	37.74 ± 10.41	12.34 ± 3.69	6.97 ± 1.89
MRT (hr)	2.79 ± 1.02	4.63 ± 1.39	4.65 ± 1.53
Vss (ml/kg)	185.98 ± 29.89	80.93 ± 14.69	49.68 ± 12.98

**Fig. 5** Plasma pharmacokientics of DIM-P and formulations after intravenous administration in Balb/c mice.
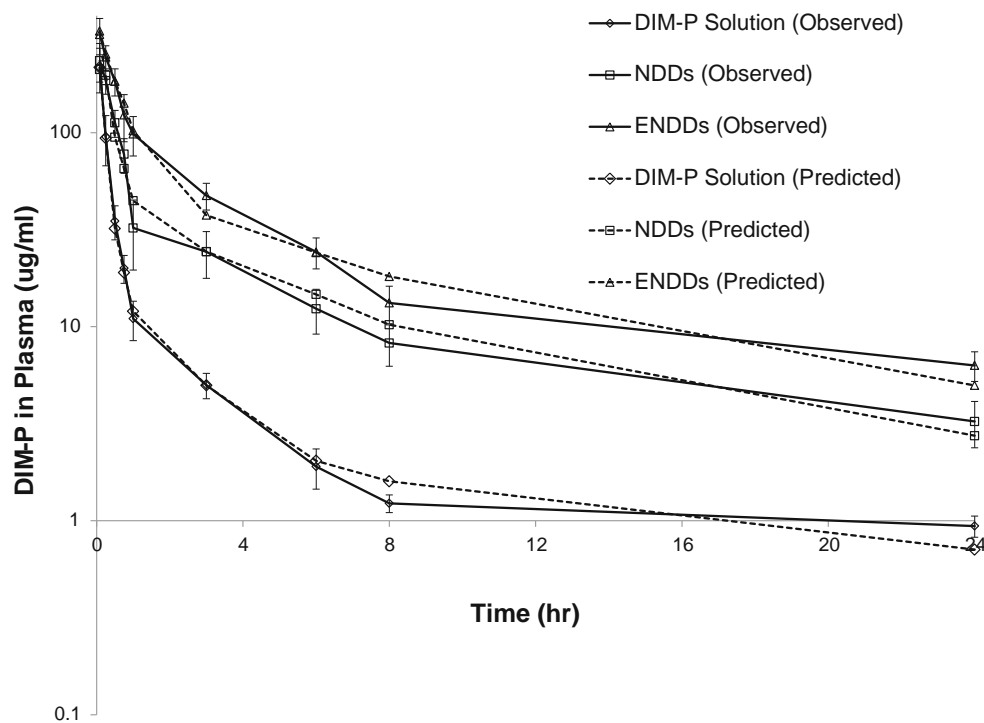
Pharmacokinetic Analysis of NDDs and ENDDs

The plasma pharmacokinetic of DIM-P solution, NDDs and ENDDs following intravenous administration are shown in Fig. 5. The plasma concentrations of DIM-P declined in a biphasic manner. The plasma drug-concentration profile following i.v. administration of DIM-P solution showed less than 2 h apparent distributional phase followed by prolonged disposition through the sampling times. However, NDDs and ENDDs plasma concentrations declined slowly compared to that of DIM-P. The primary and secondary parameters estimated following i.v. administration are shown in Table V. Based on the parameters obtained, it was obvious that nanoparticle formulations altered the pharmacokinetics of DIM-P.

In Vivo Anticancer Evaluation in Lung Cancer Models

After ten days of tumor inoculation, the average lung weight and tumor volume were 245 ± 15.89 mg and 215 ± 21.48 mm^3, respectively. Treatment was started ten days after tumor implantation and continued for a total of 35 days. The results (Fig. 6) showed that orthotopic A549 lung tumor

weights were significantly (*, $p < 0.001$) decreased after treatment with ENDDs compared to NDDs. Lung tumor volume reduction (Fig. 6) in mice treated with NDDs and ENDDs were 51.8 ± 4.3 and $79.7 \pm 6.1\%$ respectively. ENDDs treatment showed a significant (*, $p < 0.001$) decrease in average number of tumor nodules in central, mid and peripheral regions compared to NDDs and control groups. A non-significant ($p > 0.05$) change in average number of tumor nodules was observed among central, mid and peripheral regions of harvested lungs from each treated groups. We did not observe any weight loss or other signs of toxicity in mice treated with NDDs and ENDDs (Fig. 6). Also, the anticancer activity of DIM-P and Doc as NDDs and ENDDs in female athymic nude mice bearing H1650 metastatic lung tumors showed similar results (Fig. 7). Also, we analyzed wet to dry lung weight ratio (WDR) as to measure the lung edema (33). The WDR of 5.63 ± 0.71 and 5.20 ± 0.35 was found in the tumor bearing mice treated with ENDDs and NDDs. In the non-tumor bearing mice treated with ENDDs the WDR was 4.62 ± 0.56. The treatment groups showed non-significant ($p > 0.05$) difference in the WDR. Also, normal mice have a WDR in the range of 4 to 6.5 and in case of severe lung edema a value increases significantly (>6.5) (33). Thus these results
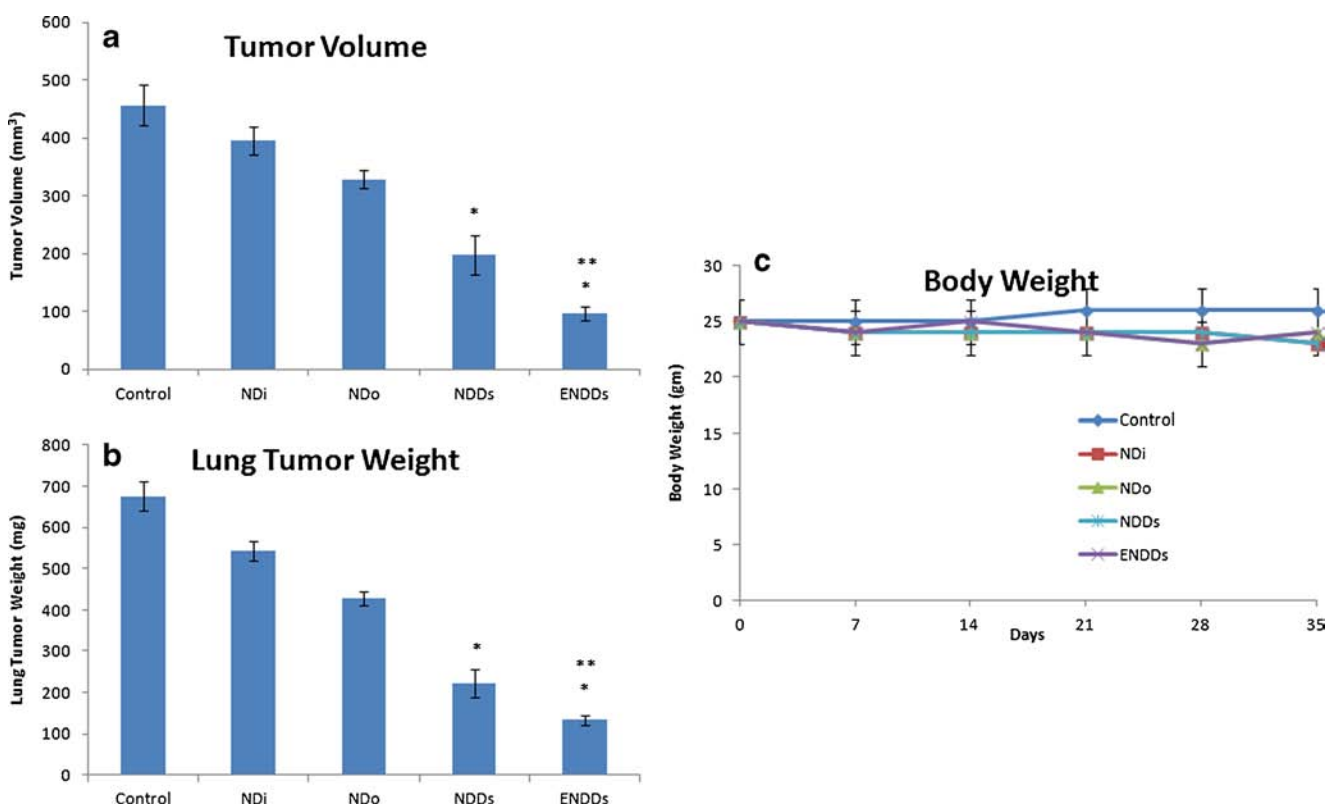
Fig. 6 Effects of NDDs and ENDDs on orthotopic A549 lung tumor weight (**a**); tumor volume (**b**); mice body weight (**c**). Lung weights and tumor volumes were determined for measurement of therapeutic activity of the treatments. Control group received blank ENDDs only. ($p < 0.05$, statistical significance of the difference in tumor volume/weight of treatment groups) (*, significantly different from controls, NDi and NDo; **, significantly different from NDDs). Data presented are means and SD ($n = 6$). This experiment was repeated twice.
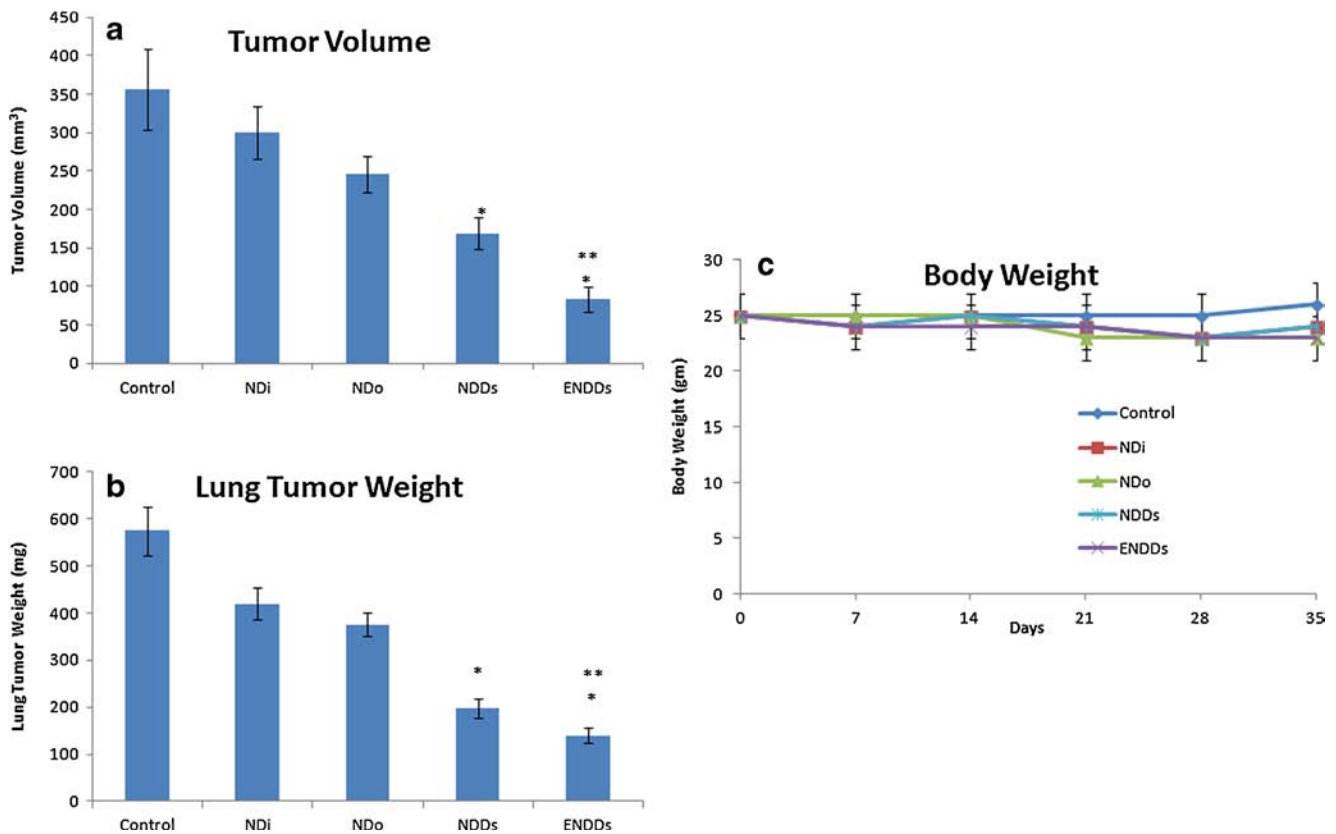
Fig. 7 Effects of NDDs and ENDDs on metastatic H1650 lung tumor weight (**a**); tumor volume (**b**); mice body weight (**c**). Lung weights and tumor volumes were determined for measurement of therapeutic activity of the treatments. Control group received blank ENDDs only. ($p < 0.05$, statistical significance of the difference in tumor volume/weight of treatment groups) (*, significantly different from controls, NDi and NDo; **, significantly different from NDDs). Data presented are means and SD ($n = 6$). This experiment was repeated twice.

confirm the lack of non-statistical difference in edema formation as a result of EphA2 activation in treatment group.

Real-Time PCR Analysis

The relative mRNA levels for PARP, caspases, Bcl-2, Bax, BAD, Mcl-1, survivin, NF-κB from formulations NDs; NDDs; and ENDDs are illustrated in Tables VI and S1. The expression trend for the proapoptotic, apoptotic and cell survival markers was the same as observed for immunohistochemistry. NDDs and ENDDs treatment significantly ($p < 0.05$) decreased PARP expression to 0.36 and 0.58-fold in regressed tumor samples compared to controls groups respectively. In regressed tumors, the ENDDs ($p < 0.001$) and NDDs ($p < 0.01$) significantly increased Cleaved Caspases - 3 expression to 0.8, and 0.4-fold, respectively (Table VI). ENDDs treatment showed increased Bax protein expression significantly ($p < 0.05$) to 0.58-fold compared to 0.32-fold NDDs ($p < 0.01$) respectively of controls in regressed tumors (Table VI). The NDDs & ENDDs decreased Bcl2 and Mcl-1 expression significantly ($p < 0.001$) compared to tumors harvested from control group (Table VI). NDDs and ENDDs treatment significantly ($p < 0.05$) decreased survivin expression in regressed

tumor samples compared to control groups respectively (Table VI). Similarly, NF-κB mRNA expression was decreased in the treatment groups.

In-Vivo Imaging of Tumors and Tracking of NDDs and ENDDs

In-vivo imaging of tumors and tracking of NDs was performed using luciferase system (NDDs/ENDDs) with Carestream *In-Vivo* MS FX PRO. *In-vivo* imaging following exposure of NDDs/ENDDs demonstrated their targeting to the tumors (Fig. 8), where the ENDDs were found to be migrating more to tumors with total radiant efficiency [p/s]/[μW/cm²] of $9.1*10^{11} \pm 1.5*10^{11}$ compared to NDDs with total radiant efficiency [p/s]/[μW/cm²] of $0.2*10^{10} \pm 0.18*10^{10}$ over the period of 0.5 h to 3 h.

DISCUSSION

Variety of nanoparticle systems currently being explored for cancer therapeutics (14) include dendrimers, liposomes,

Table VI Relative mRNA Expression Levels by RT-PCR: Real-time PCR was Performed and the mRNA Expression Levels of Different Proteins Normalized by β-actin were Investigated for Tumor Tissues. Data Represent Mean ± SD, $n = 6$

|	NF-kB	Mdl-I	Bax	Bcl-2	Caspase-8	Cleaved caspase-3	Survivin	BAD	PARP	VEGF	Akt
Con	1.04±0.09	1.32±0.08	0.76±0.04	1.16±0.11	0.48±0.11	0.46±0.06	1.13±0.13	0.70±0.08	1.25±0.06	1.21±0.10	1.15±0.07
NDi	0.80±0.06	1.07±0.06	0.83±0.03	0.85±0.08	0.55±0.05	0.54±0.05	1.03±0.11	0.89±0.04	1.07±0.05	0.92±0.09	0.97±0.08
NDo	0.69±0.09	0.88±0.08	0.94±0.08	0.66±0.06	0.65±0.01	0.60±0.01	0.95±0.09	0.97±0.07	0.96±0.11	0.76±0.06	0.82±0.10
NDDs	0.67±0.10	0.63±0.12	0.99±0.10	0.58±0.05	0.73±0.01	0.70±0.02	0.87±0.11	1.07±0.07	0.79±0.03	0.62±0.09	0.60±0.09
ENDDs	0.38±0.02**	0.52±0.09	1.21±0.09	0.39±0.03**	0.83±0.03**	0.85±0.03**	0.62±0.09	1.20±0.06	0.58±0.07**	0.47±0.05	0.46±0.07

**, $p < 0.05$ significantly different than NDDs

polymeric, metallic, ceramic or viral nanoparticles, micelles, and carbon nanotubes. Efforts are ongoing to improve the clinical response by using synergistically acting drugs in cancer patients. The receptor specific targeted delivery of combination drugs using nanotechnology based formulations is essential to improve the clinical outcome for lung cancer. In this study, we have developed a novel theranostic approach for treatment and imaging of lung cancer using targeted multi-functional ENDDs and is the first report of combining two anticancer agents in a nanoparticle which are targeted to the Epha2 receptor on lung tumor cells. The NDs formulations were formulated using different lipids and surface of NDDs was modified using specific groups like DOGS-NTA. Thus, we have utilized a rational approach in designing stable and multifunctional NDs and evaluated its efficacy against lung cancer.

The *in-vitro* analysis showed that optimizes NDDs were < 200 nm in size and released the drug content (DIM-P/Doc) by zero order kinetics from NDDs. Also, cytotoxicity analysis showed >98% viability of A549 cells with placebo NDs/ ENDDs showing non-toxicity of the excipient used in the preparation of formulations.

Followed by *in-vitro* analysis of NDDs treatment, the efficacy of NDs as a single therapeutic agent and in combination with Doc (NDDs) against lung tumors was evaluated. In the present study, the delivery of NDDs [5 mg/kg DIM-P equivalent and Doc (2 mg/kg)] showed significant ($p < 0.01$) reduction in tumor growth compared to the single agent treatment (Fig. 8). The ENDDs further improved the effectiveness due to targeted delivery of ENDDs and significant ($p < 0.01$) inhibition of lung tumor growth compared to control and NDDs. It is likely that other tumor types can be similarly targeted, because other researchers have shown other types of tumors can be targeted using EphA2 peptide (29,30). Consistent with anti-tumor activity, DIM-P/Doc bio-distribution studies demonstrated that ENDDs provided a significant increase in the amount of drug delivered to the tumor compared with administration of free DIM-P/Doc. ENDDs prolonged the half-life of DIM-P, as shown by pharmacokinetic analysis which was substantiated by imaging of ENDDs *in vivo*. The PEGylation of ENDDs is most likely responsible for this, since its hydrophilicity, flexibility, and neutral charge in biological fluids helps in their dispersion and increases their blood circulation times (37–40). There is no statistically significant difference between NDDs and ENDDs in term of pharmacokinetic half-life (circulation of drug in blood). Since, EphA2 is highly overexpressed in tumor cells, in tumor bearing mice, the targeting becomes more apparent as we see in our pharmacodynamic studies. Thus ENDDs is targeting the tumor cells *via* EphA2 targeting.

The tumor targeting and tumor tissue penetration traits of ENDDs most likely reasons for enhanced anti-tumor activity. ENDDs selectively bind to EphA2 due to YSA peptide on
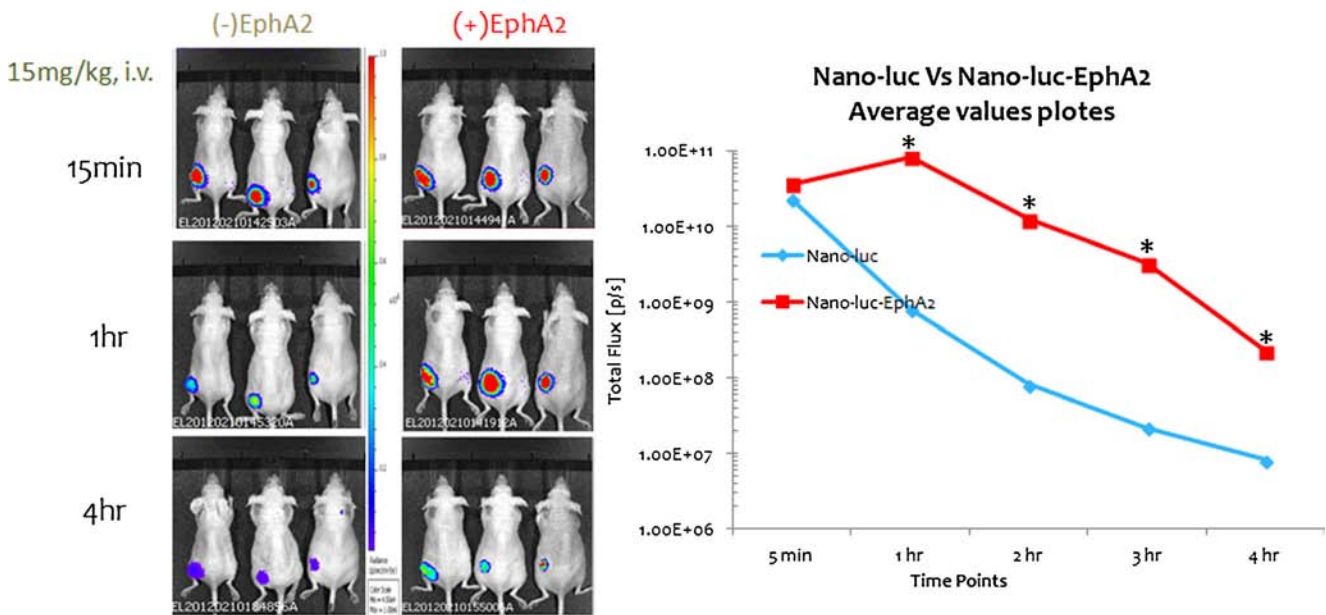
Fig. 8 Tumor Imaging in mice with orthotopic 4T1-luc2 tumors using 15 mg/kg luciferin equivalent NDDs and ENDDs. (**a**) Bioluminescent signals taken at different time point in a 4T1-luc model. (**b**) Total flux of bioluminescence Vs time plot following IV injection of NDDs and ENNDs. ($p < 0.05$, statistical significance of the difference in total flux of treatment groups) (*, significantly different from (NDDs) Nano-luc). Data presented are means average ($n = 3$). This experiment was repeated twice.

surface of NDDs, leading to internalization of the EphA2-ENDDs complex and actively transports DIM-P/Doc into cells, leading to a significant decrease in tumor growth. Similar to these findings, Scarberry *et al.* reported the use magnetic cobalt ferrite nanoparticles coated with the YSA peptide to target EphA2 expressing ovarian carcinoma cells (28). Similarly, Wang et al showed doxorubicin stealth liposomes made with YSA coupled lipids as a therapy system for Choroidal neovascularization in rats (41). Furthermore, Wykosky et al (42) and Sun et al (43) showed dose-dependent killing of cancer cells by conjugating an exotoxin to the natural EphA2 ligand. Alternatively, Jackson et al (44) developed an EphA2 monoclonal antibody conjugate to target tumors expressing high levels of EphA2. Similarly, Wamg et al (45) showed effective targeting of YSA-paclitaxel conjugate to prostate cancer. However, protein-based therapeutic strategies still have the drawbacks (*e.g.* immunogenic or allergic responses). Thus, it is advantageous to use peptide that selectively bind to EphA2 and use its ability to mediate internalization (46). The normal tissues have low EphA2 expression compare to tumor tissues and based on our bio-distribution data, the use of the YSA peptide for drug delivery may reduce toxic side-effects by reducing exposure of cytotoxic drugs to normal cells.

Previous *in vitro* studies with A549 and H460 lung cancer cells in our laboratory demonstrated that the combination of DIM-P + Doc synergistically or additively induced apoptosis and several proapoptotic proteins. Moreover, Ichite et al (5), *in vivo* studies, using Doc (i.v. bolus 10 mg/kg) and DIM-P

(40 mg/kg) three times weekly by oral gavage showed that both compounds alone and in the combination induced apoptosis and decreased lung weights (compared to vehicle control). Previous studies with DIM-P and related C-substituted DIMs demonstrated that these compounds induce multiple pro-apoptotic responses that activate the intrinsic and extrinsic pathways. In addition other proteins such as cyclin D1 and the estrogen receptor are downregulated by c-substituted DIM through activation of the proteasome pathway. Further, C-substituted DIMs also enhance or modulate phosphorylation of several kinases including JNK. Result of our *in vivo* studies demonstrate that NDs, NDDs and ENDDs treatment induce proapototic (Bax) or decrease survival (survivin, Akt and Mcl-1) proteins and this was also accompanied by downregulation of Bcl2 (Table VI). Ichite et al reported reduction in VEGF and CD31 expression in A549 lung orthotropic tumors treated with combination of DIM-P and Doc (47). Similarly, We observed decreased expression of VEGF in lung tumors from mice treated with ENDDs compared to those treated with NDs and NDDs or control in regressed tumors.

In the tumor tissue, the molecular changes as a result of anticancer therapy usually happens before any anatomical changes can be detected. Thus, some researchers have used non-invasive imaging of EphA2 expression (highly expressed in tumors) as a means to measure anti-EphA2 cancer therapy. Cai et al. (48) used humanized monoclonal antibody (ICI) conjugated to 64Cu through DOTA for quantitative radioimmunoPET imaging of EphA2 in tumors. Similar to

Cai et al., Scarberry et al. (28) used YSA peptide conjugated magnetic iron oxide nanoparticle for ovarian cancer imaging and removal of metastatic cancer cells from the fluid of the abdominal cavity or circulatory system. We used whole body imaging using a bioluminescent system (luciferin) and NIR flourescent (Xenolight DiR) instead of DIM-P to ascertain feasibility of ENDDs as diagnostic tool for possible theranostic application. *In-vivo* imaging using bioluminescent system with ENDDs showed local concentration of ENDDs at tumors was almost 60 fold higher than NDDs in terms of radiant efficiency flux. Furthermore, we were able to monitor the effect of therapy at molecular level and quantify flux intensity. These results shows the possible theranostic application of ENDDs in management of lung cancer treatment.

CONCLUSION

In summary, a tumor targeted stable nano-carrier was effectively developed for delivery of DIM-P and Doc. Our results suggest that the efficacy of DIM-P and Doc was enhanced with use of ENDDs compared to non-targeted NDDs and single agent NDs formulations. In addition, our approach of using ENDDs for delivery of DIM-P & Doc could overcome the PK limitations and reduce toxicities of Doc, while improving the therapeutic outcome of lung cancer treatment. Our *in vitro* and *in vivo* results demonstrate that ENDDs inhibits tumor growth by multiple pathways. Using NIR fluorescent and bioluminescent *in vivo* imaging, we were able to track and evaluate the targetability of ENDDs to lung tumors.

REFERENCES

1. Fleming S, Lucas F, Schofield M. A therapeutic area review of oncology products and players. Expert Opin Emerg Drugs. 2001;6(2):317–29.
2. Douillard JY, Eckardt J, Scagliotti GV. Challenging the platinum combinations in the chemotherapy of NSCLC. Lung Cancer. 2002;38 Suppl 4:21–8.
3. Tseng CL, Wu SY, Wang WH, Peng CL, Lin FH, Lin CC, *et al.* Targeting efficiency and biodistribution of biotinylated-EGF-conjugated gelatin nanoparticles administered via aerosol delivery in nude mice with lung cancer. Biomaterials. 2008;29(20):3014–22.
4. Chintharlapalli S, Smith 3rd R, Samudio I, Zhang W, Safe S. 1,1-Bis(3′-indolyl)-1-(p-substitutedphenyl)methanes induce peroxisome proliferator-activated receptor gamma-mediated growth inhibition, transactivation, and differentiation markers in colon cancer cells. Cancer Res. 2004;64(17):5994–6001.
5. Ichite N, Chougule MB, Jackson T, Fulzele SV, Safe S, Singh M. Enhancement of docetaxel anticancer activity by a novel diindolylmethane compound in human non-small cell lung cancer. Clin Cancer Res. 2009;15(2):543–52.
6. Kassouf W, Chintharlapalli S, Abdelrahim M, Nelkin G, Safe S, Kamat AM. Inhibition of bladder tumor growth by 1,1-bis(3′-indolyl)-1-(p-substitutedphenyl)methanes: a new class of peroxisome proliferator-activated receptor gamma agonists. Cancer Res. 2006;66(1):412–8.
7. Chintharlapalli S, Papineni S, Safe S. 1,1-Bis(3′-indolyl)-1-(p-substituted phenyl)methanes inhibit colon cancer cell and tumor growth through PPARgamma-dependent and PPARgamma-independent pathways. Mol Cancer Ther. 2006;5(5):1362–70.
8. Su Y, Vanderlaag K, Ireland C, Ortiz J, Grage H, Safe S, *et al.* 1,1-Bis(3′-indolyl)-1-(p-biphenyl)methane inhibits basal-like breast cancer growth in athymic nude mice. Breast Cancer Res. 2007;9(4):R56.
9. Horn L, Visbal A, Leighl NB. Docetaxel in non-small cell lung cancer: impact on quality of life and pharmacoeconomics. Drugs Aging. 2007;24(5):411–28.
10. Wakelee H, Belani CP. Optimizing first-line treatment options for patients with advanced NSCLC. Oncologist. 2005;10 Suppl 3:1–10.
11. van Zuylen L, Verweij J, Sparreboom A. Role of formulation vehicles in taxane pharmacology. Invest New Drugs. 2001;19(2):125–41.
12. Engels FK, Mathot RA, Verweij J. Alternative drug formulations of docetaxel: a review. Anticancer Drugs. 2007;18(2):95–103.
13. Heath JR, Davis ME. Nanotechnology and cancer. Annu Rev Med. 2008;59:251–65.
14. Peer D, Karp JM, Hong S, Farokhzad OC, Margalit R, Langer R. Nanocarriers as an emerging platform for cancer therapy. Nat Nanotechnol. 2007;2(12):751–60.
15. Sung JC, Pulliam BL, Edwards DA. Nanoparticles for drug delivery to the lungs. Trends Biotechnol. 2007;25(12):563–70.
16. Wong HL, Bendayan R, Rauth AM, Li Y, Wu XY. Chemotherapy with anticancer drugs encapsulated in solid lipid nanoparticles. Adv Drug Deliv Rev. 2007;59(6):491–504.
17. Noblitt LW, Bangari DS, Shukla S, Knapp DW, Mohammed S, Kinch MS, *et al.* Decreased tumorigenic potential of EphA2-overexpressing breast cancer cells following treatment with adenoviral vectors that express EphrinA1. Cancer Gene Ther. 2004;11(11):757–66.
18. Zelinski DP, Zantek ND, Stewart JC, Irizarry AR, Kinch MS. EphA2 overexpression causes tumorigenesis of mammary epithelial cells. Cancer Res. 2001;61(5):2301–6.
19. Brantley-Sieders DM, Zhuang G, Hicks D, Fang WB, Hwang Y, Cates JM, *et al.* The receptor tyrosine kinase EphA2 promotes mammary adenocarcinoma tumorigenesis and metastatic progression in mice by amplifying ErbB2 signaling. J Clin Invest. 2008;118(1):64–78.
20. Vaught D, Brantley-Sieders DM, Chen J. Eph receptors in breast cancer: roles in tumor promotion and tumor suppression. Breast Cancer Res. 2008;10(6):217.
21. Brannan JM, Dong W, Prudkin L, Behrens C, Lotan R, Bekele BN, *et al.* Expression of the receptor tyrosine kinase EphA2 is increased in smokers and predicts poor survival in non-small cell lung cancer. Clin Cancer Res. 2009;15(13):4423–30.
22. Kamat AA, Coffey D, Merritt WM, Nugent E, Urbauer D, Lin YG, *et al.* EphA2 overexpression is associated with lack of hormone receptor expression and poor outcome in endometrial cancer. Cancer. 2009;115(12):2684–92.
23. Holm R, de Putte GV, Suo Z, Lie AK, Kristensen GB. Expressions of EphA2 and EphrinA-1 in early squamous cell cervical carcinomas and their relation to prognosis. Int J Med Sci. 2008;5(3):121–6.
24. Herath NI, Spanevello MD, Sabesan S, Newton T, Cummings M, Duffy S, *et al.* Over-expression of Eph and ephrin genes in advanced ovarian cancer: ephrin gene expression correlates with shortened survival. BMC Cancer. 2006;6:144.
25. Yang P, Yuan W, He J, Wang J, Yu L, Jin X, *et al.* Overexpression of EphA2, MMP-9, and MVD-CD34 in hepatocellular carcinoma: implications for tumor progression and prognosis. Hepatol Res. 2009;39(12):1169–77.

26. Shao Z, Zhang WF, Chen XM, Shang ZJ. Expression of EphA2 and VEGF in squamous cell carcinoma of the tongue: correlation with the angiogenesis and clinical outcome. Oral Oncol. 2008;44(12): 1110–7.

27. Fang WB, Brantley-Sieders DM, Hwang Y, Ham AJ, Chen J. Identification and functional analysis of phosphorylated tyrosine residues within EphA2 receptor tyrosine kinase. J Biol Chem. 2008;283(23):16017–26.

28. Scarberry KE, Dickerson EB, McDonald JF, Zhang ZJ. Magnetic nanoparticle-peptide conjugates for in vitro and in vivo targeting and extraction of cancer cells. J Am Chem Soc. 2008;130(31):10258–62.

29. Koolpe M, Dail M, Pasquale EB. An ephrin mimetic peptide that selectively targets the EphA2 receptor. J Biol Chem. 2002;277(49): 46974–9.

30. Lee JW, Han HD, Shahzad MM, Kim SW, Mangala LS, Nick AM, et al. EphA2 immunoconjugate as molecularly targeted chemotherapy for ovarian carcinoma. J Natl Cancer Inst. 2009;101(17):1193–205.

31. Afar DE, Bhaskar V, Ibsen E, Breinberg D, Henshall SM, Kench JG, et al. Preclinical validation of anti-TMEFF2-auristatin E-conjugated antibodies in the treatment of prostate cancer. Mol Cancer Ther. 2004;3(8):921–32.

32. Qin C, Morrow D, Stewart J, Spencer K, Porter W, Smith 3rd R, et al. A new class of peroxisome proliferator-activated receptor gamma (PPARgamma) agonists that inhibit growth of breast cancer cells: 1,1-Bis(3′-indolyl)-1-(p-substituted phenyl)methanes. Mol Cancer Ther. 2004;3(3):247–60.

33. Patel AR, Chougule MB, Townley I, Patlolla R, Wang G, Singh M. Efficacy of aerosolized celecoxib encapsulated nanostructured lipid carrier in non-small cell lung cancer in combination with docetaxel. Pharm Res. 2013;30(5):1435–46.

34. Patlolla RR, Chougule M, Patel AR, Jackson T, Tata PN, Singh M. Formulation, characterization and pulmonary deposition of nebulized celecoxib encapsulated nanostructured lipid carriers. J Control Release. 2010;144(2):233–41.

35. Patlolla RR, Desai PR, Belay K, Singh MS. Translocation of cell penetrating peptide engrafted nanoparticles across skin layers. Biomaterials. 2010;31(21):5598–607.

36. Patel AR, Spencer SD, Chougule MB, Safe S, Singh M. Pharmacokinetic evaluation and in vitro-in vivo correlation (IVIVC) of novel methylene-substituted 3,3′ diindolylmethane (DIM). Eur J Pharm Sci. 2012;46(1–2):8–16.

37. Lim SM, Kim TH, Jiang HH, Park CW, Lee S, Chen X, et al. Improved biological half-life and anti-tumor activity of TNF-related apoptosis-inducing ligand (TRAIL) using PEG-exposed nanoparticles. Biomaterials. 2011;32(13):3538–46.

38. Moghimi SM, Hunter AC, Murray JC. Long-circulating and target-specific nanoparticles: theory to practice. Pharmacol Rev. 2001;53(2): 283–318.

39. Zhu S, Hong M, Tang G, Qian L, Lin J, Jiang Y, et al. Partly PEGylated polyamidoamine dendrimer for tumor-selective targeting of doxorubicin: the effects of PEGylation degree and drug conjugation style. Biomaterials. 2010;31(6):1360–71.

40. Fang YP, Wu PC, Huang YB, Tzeng CC, Chen YL, Hung YH, et al. Modification of polyethylene glycol onto solid lipid nanoparticles encapsulating a novel chemotherapeutic agent (PK-L4) to enhance solubility for injection delivery. Int J Nanomedicine. 2012;7:4995–5005.

41. Wang JL, Liu YL, Li Y, Dai WB, Guo ZM, Wang ZH, et al. EphA2 targeted doxorubicin stealth liposomes as a therapy system for choroidal neovascularization in rats. Invest Ophthalmol Vis Sci. 2012;53(11):7348–57.

42. Wykosky J, Gibo DM, Debinski W. A novel, potent, and specific ephrinA1-based cytotoxin against EphA2 receptor expressing tumor cells. Mol Cancer Ther. 2007;6(12 Pt 1):3208–18.

43. Sun XL, Xu ZM, Ke YQ, Hu CC, Wang SY, Ling GQ, et al. Molecular targeting of malignant glioma cells with an EphA2-specific immunotoxin delivered by human bone marrow-derived mesenchymal stem cells. Cancer Lett. 2011;312(2):168–77.

44. Jackson D, Gooya J, Mao S, Kinneer K, Xu L, Camara M, et al. A human antibody-drug conjugate targeting EphA2 inhibits tumor growth in vivo. Cancer Res. 2008;68(22):9367–74.

45. Wang S, Placzek WJ, Stebbins JL, Mitra S, Noberini R, Koolpe M, et al. Novel targeted system to deliver chemotherapeutic drugs to EphA2-expressing cancer cells. J Med Chem. 2012;55(5):2427–36.

46. Noberini R, Lamberto I, Pasquale EB. Targeting Eph receptors with peptides and small molecules: progress and challenges. Semin Cell Dev Biol. 2012;23(1):51–7.

47. Ichite N, Chougule M, Patel AR, Jackson T, Safe S, Singh M. Inhalation delivery of a novel diindolylmethane derivative for the treatment of lung cancer. Mol Cancer Ther. 2010;9(11):3003–14.

48. Weibo C, Alireza E, Kai C, Qizhen C, Zi-Bo L, David AT, Xiaoyuan C. Quantitative radioimmuno PET imaging of EphA2 in tumor-bearing mice. Eur J Nucl Med Mol Imag. 2007;34(12): 2024–2036.